Design and Performance Prediction of Space Vector-Based PMU Algorithms

Sergio Toscani, *Member, IEEE*, Carlo Muscas, *Senior Member, IEEE*, and Paolo Attilio Pegoraro, *Member, IEEE*

***Abstract*— Phasor measurement units (PMUs) are expected to be the basis of modern power networks monitoring systems. They are conceived to allow measuring the phasor, frequency, and rate of change of frequency (ROCOF) of electrical signals in a synchronized way and with unprecedented accuracy. PMUs are intended to apply to three-phase systems and to track signal parameters evolution during network dynamics. For these reasons, the design of the algorithms and, in particular, of the filters that allow rejecting the disturbances while preserving the passband signal content is a paramount concern. In this paper, a novel space vector approach is proposed. It exploits the three-phase nature of the monitored signals together with proper lowpass and differentiation filters. Analytical formulas for performance prediction under almost all the test conditions prescribed by the synchrophasor standard C37.118.1 for PMUs, are introduced. The given expressions are extremely accurate, thus allowing to derive the filter design criteria for phasor, frequency, and ROCOF computation, so that the requirements in terms of estimation errors can be easily translated into filter specifications. The implications of the proposed approach in practical PMU design are illustrated by means of two simple design examples matching P and M compliance classes, respectively, for all the test cases of the standard. The reported performance proves the validity of the proposal.**

***Index Terms*— Digital filters, phasor measurement units (PMUs), space vector (SV), voltage measurement.**

I. Introduction

PHASOR measurement units (PMUs) are going to become the cornerstone of the monitoring systems of electric power networks, due to their capacity to measure voltage and current phasors with respect to an absolute coordinated universal time (UTC) reference. PMUs have better accuracy and higher reporting rates (up to 50–100 frames/s for a fundamental frequency of 50 Hz) than conventional measurement devices.

Requirements for synchrophasor, frequency, and rate of change of frequency (ROCOF) measurement accuracies have been, for instance, set in the IEEE C37.118.1 standard [1], which, along with its amendment IEEE C37.118.1a [2], fixes the limits for the total error vector (TVE), absolute frequency error (FE), and absolute ROCOF error (RFE) of PMU measurements under specific tests. The adopted test signals are designed to stress the PMU behavior under different conditions, thus covering both steady-state (off-nominal frequency conditions, harmonic and interharmonic disturbances) and dynamic operation (amplitude and phase-angle modulations, frequency ramps and steps in both amplitude and phase). The standard defines two accuracy classes for PMU compliance: P class, for protection applications, and M class, for measurement applications.

In recent years, great attention has been paid by the scientific community to algorithms for synchrophasor, frequency, and ROCOF measurements, that are able to cope with different conditions and, in particular, with the dynamic conditions electrical signals can undergo in real applications. A wide range of techniques have been employed: phase-locked loop [3], Taylor expansion of phasor model [4], [5], two channel dynamic model matching with condition detection [6], [7], interpolated DFT [8], and its extension to dynamic conditions [9], demodulation and filtering approach [10], Kalman filtering [11], [12], and compressive sensing [13]. Such algorithms rely on different models of the measured signal, trying to deal with typical conditions occurring in real applications. A detailed discussion on the algorithms and their peculiarities can be found in [14]. However, the common idea of dynamic synchrophasor measurements is to extract the bandpass signal of interest around the fundamental frequency, while rejecting unwanted disturbances.

Even if many different algorithms are proposed in the literature, much less attention is paid to PMU design and, in particular, to the three-phase nature of the signals. The most widespread approach in PMU implementation employs a filtering stage for each phase after having reported the components of interest to baseband frequencies.

The standard itself suggests (Annex C) algorithms to compute synchrophasor, frequency, and ROCOF in compliance with P and M classes based on this paradigm. In [15], the design criteria of the required filters are presented, while in [16], filter mask design for M-class compliance, for both the standard architecture and the frequency tracking one, is discussed.

In [17], a space vector (SV) approach for positive sequence synchrophasor and frequency estimation characterized by an extremely low computational burden was introduced. IIR filters were adopted, while magnitude, phase, and fre-

Manuscript received July 6, 2016; revised October 10, 2016; accepted November 24, 2016. Date of publication December 29, 2016; date of current version February 8, 2017. The Associate Editor coordinating the review process was Dr. Octavian Postolache.

S. Toscani is with the Dipartimento di Elettronica, Informazione e Bioingegneria, Politecnico di Milano, Piazza Leonardo da Vinci 32, 20133 Milan, Italy (e-mail: sergio.toscani@polimi.it).

C. Muscas and P. A. Pegoraro are with the Department of Electrical and Electronic Engineering, University of Cagliari, Piazza d'Armi, 09123 Cagliari, Italy (e-mail: carlo@diee.unica.it; paolo.pegoraro@diee.unica.it).

Color versions of one or more of the figures in this paper are available online at http://ieeexplore.ieee.org.

quency were obtained by least squares (LSs) interpolation.

In this paper, the SV approach is generalized and extended to the complete design of the estimation algorithm for synchrophasor, frequency, and ROCOF. Disturbances are rejected by proper FIR filters and analytical expressions, derived for the proposed architecture, permit to predict the results of almost all the compliance tests required by the standard. On the other hand, these equations allow translating the requirements in terms of TVE, FE, and RFE into filter design specifications. The high accuracy achieved by such expressions is shown, and examples of filter designs for P-class and M-class compliance are reported to illustrate the potentialities of the method. The algorithm is computationally light and allows the tradeoff between accuracy and speed to be straightforwardly implemented for each specific application.

II. Measurement Model and Conventional Approach

The definition of synchrophasor is reported in [1], starting from the time-domain expression of a generic ac signal. In this respect, let us consider a three-phase system characterized by its rated frequency f_0 and rated angular frequency ω_0. Using the vector notation, a three-phase quantity $\boldsymbol{x}_{abc}$ (that is typically represented by a set of three-phase node voltages or line currents) can be written as the sum of a fundamental component $\boldsymbol{x}_{1,abc}$ and a disturbance $\boldsymbol{d}_{abc}$

$$\boldsymbol{x}_{abc}(t) = \boldsymbol{x}_{1,abc}(t) + \boldsymbol{d}_{abc}(t). \tag{1}$$

The letters a, b, and c are employed to denote the phases of the power system. For each phase, the main component is given by

$$x_{1,p}(t) = \sqrt{2} X_{1,p} \cos\left[\theta_1(t) + \varphi_{1,p}\right] \tag{2}$$

where $X_{1,p}$ is the rms value of the component, $\varphi_{1,p}$ its phase angle, and $p \in \{a, b, c\}$. In (2), the monotonically increasing angle θ_1 has been introduced. It can be expressed as

$$\theta_1(t) = \int_0^t \omega_1(t')dt' \tag{3}$$

with respect to a reference time instant, in this case, $t = 0$.

The angular frequency $\omega_1 > 0$, namely, the derivative of the angle θ_1, is always close to the rated value ω_0. Even if it is not evident from the equations,[1] both the rms value $X_{1,p}$ and the angular frequency ω_1 depend on time; however, their rate of change is much slower when compared with ω_0.

The disturbance introduced in (1) can be decomposed into the sum of several spectral components, each one characterized by a different frequency (as in the compliance tests [1]). In terms of phase quantities

$$\begin{aligned} d_p(t) = X_{0,p} &+ \sum_{k=2}^{\infty} \sqrt{2} X_{k,p} \cos[k\theta_1(t) + \varphi_{k,p}] \\ &+ \sum_{k=1}^{\infty} \sqrt{2} X_{nh,k,p} \cos[\theta_{nh,k}(t) + \varphi_{nh,k,p}]. \end{aligned} \tag{4}$$

[1]The time dependence of the variables is here explicitly indicated only when their rate of change is significant with respect to ω_0.

$X_{0,p}$ represents the unidirectional component. The first sum considers the harmonic disturbances, namely, sinusoidal terms whose frequencies are integer multiples of ω_1. The second sum takes into account nonharmonic (subharmonics and interharmonics) disturbances. Similar to θ_1, the monotonic increasing angle $\theta_{nh,k}$ is defined as

$$\theta_{nh,k}(t) = \int_0^t \omega_{nh,k}(t')dt'. \tag{5}$$

By definition, the ratio between $\omega_{nh,k} > 0$ and ω_1 is not an integer.

Now let us consider again the main component; using the Euler's formula, (2) can be rewritten as

$$x_{1,p}(t) = \sqrt{2}\Re[\bar{X}_{1,p}\, e^{j\theta_1(t)}] \tag{6}$$

having introduced $\bar{X}_{1,p} = X_{1,p} e^{j\varphi_{1,p}}$ as the phasor of the fundamental component (the symbol $\Re$ denotes the real part operator). The same applies to the disturbances

$$\begin{aligned} d_p(t) = X_{0,p} + \sqrt{2}\Re\Bigg[&\sum_{k=2}^{\infty} \bar{X}_{k,p}\, e^{jk\theta_1(t)} \\ &+ \sum_{k=1}^{\infty} \bar{X}_{nh,k,p}\, e^{j\theta_{nh,k}(t)} \Bigg]. \end{aligned} \tag{7}$$

$\bar{X}_{k,p} = X_{k,p} e^{j\varphi_{k,p}}$ and $\bar{X}_{nh,k,p} = X_{nh,k,p} e^{j\varphi_{nh,k,p}}$ are the phasors of the generic harmonic and nonharmonic component, respectively.

From (6) and (7), a phase quantity is expressed as sum of rotating vectors projected on the real axis of a stationary reference frame; the phasor of each rotating vector expresses its magnitude and initial phase. On the other hand, from [1], the synchrophasors $\bar{X}_{1,a,S}$, $\bar{X}_{1,b,S}$, and $\bar{X}_{1,c,S}$ of the phase quantities x_a, x_b, and x_c can be defined as projections of the rotating vectors of the respective fundamental components on a common reference frame rotating at ω_0 (the rated angular frequency of the power system) synchronized to UTC. Using the vector notation, this leads to

$$\bar{\boldsymbol{X}}_{1,abc,S}(t) = \bar{\boldsymbol{X}}_{1,abc} e^{j[\theta_1(t) - \beta(t)]} \tag{8}$$

β represents the instantaneous angular position of the reference frame, whose derivative is ω_0. An ideal synchrophasor estimation algorithm should perfectly reject the disturbing term, extract the phasor of the main component, and compute its projection on the synchronous reference frame. Most of the techniques are based on the formal definition of phasor, thus on the Steinmetz transform: this means computing the Fourier coefficient of the main component. After that, the reference frame has to be changed in order to obtain the synchrophasor. Unfortunately, this approach, which appears to be the most straightforward, is antithetic to the concept of "dynamic phasor" introduced by [1], since it assumes periodic steady-state operation characterized by a fundamental frequency which has to be known in advance.

III. Space Vector Approach

Many applications, such as state estimation of transmission networks, only require to measure the positive sequence synchrophasor $\bar{X}_{1,+,S}$. Usually, the synchrophasors of the phase

quantities are first measured, and the positive sequence component is extracted by applying the Fortescue transformation

$$\bar{X}_{1,+,S}(t) = \frac{\bar{\boldsymbol{S}}}{\sqrt{3}}\,\bar{\boldsymbol{X}}_{1,abc,S}(t)$$
$$\bar{\boldsymbol{S}} = [\,1 \quad \bar{\alpha} \quad \bar{\alpha}^2\,] \tag{9}$$

being $\bar{\alpha} = e^{j2\pi/3}$. Using (8), (9) can be rewritten as

$$\bar{X}_{1,+,S}(t) = \frac{\bar{\boldsymbol{S}}}{\sqrt{3}}\,\bar{\boldsymbol{X}}_{1,abc}\,e^{j[\theta_1(t)-\beta(t)]} = \bar{X}_{1,+}\,e^{j[\theta_1(t)-\beta(t)]} \tag{10}$$

where $\bar{X}_{1,+}$ represents the positive sequence phasor of the main component. Equation (10) shows that the positive sequence synchrophasor represents the projection of the positive sequence rotating vector on the common, UTC-synchronized reference frame. This reminds a technique that was developed for the study of rotating electrical machines, but that can be applied to generic three-phase quantities: the SV transformation. In particular, it has been employed by Toscani and Muscas [17] for synchrophasor estimation. Starting from the time-domain expressions of the phase quantities, the SV $\bar{x}$ in a *d-q* reference frame rotating at the angular speed ω_0 results

$$\bar{x}(t) = x_d(t) + jx_q(t) = \sqrt{\frac{2}{3}}\,\bar{\boldsymbol{S}}\,\boldsymbol{x}_{abc}\,e^{-j\beta(t)}. \tag{11}$$

Using (6) and (7), while reminding that the real part is equal to half of the sum between a complex and its conjugate, it is possible to obtain

$$\bar{x}(t) = \sum_{k=-\infty}^{\infty}\bar{X}_k\,e^{j[k\theta_1(t)-\beta(t)]} + \sum_{\substack{k=-\infty\\k\neq 0}}^{\infty}\bar{X}_{nh,k}\,e^{j[\mathrm{sgn}\,(k)\theta_{nh,|k|}(t)-\beta(t)]}. \tag{12}$$

It is worth noticing that for $k > 0$, $\bar{X}_k$ is equal to $\bar{X}_{k,+}$, and hence, the positive sequence phasor of the *kth* order harmonic, where $\bar{X}_{nh,k}$ is the positive sequence phasor of the *kth* nonharmonic component, i.e., $\bar{X}_{nh,k,+}$. Similarly, when $k < 0$, $\bar{X}_k$ and $\bar{X}_{nh,k}$ correspond to $\bar{X}^*_{k,-}$ and $\bar{X}^*_{nh,k,-}$, namely, the complex conjugates of the $|k|th$ order harmonic and $|k|th$ nonharmonic component negative sequence phasors, respectively [18]. Summarizing

$$\begin{cases}\bar{X}_k = \bar{X}_{k,+}; & \bar{X}_{nh,k} = \bar{X}_{nh,k,+} \quad k > 0\\ \bar{X}_k = \bar{X}^*_{k,-}; & \bar{X}_{nh,k} = \bar{X}^*_{nh,k,-} \quad k < 0.\end{cases} \tag{13}$$

From (12), the SV is the sum of harmonic and nonharmonic synchrophasors rotating with different speeds. For each one, the absolute value of this speed corresponds to the angular frequency of its real and imaginary parts, possibly slightly modulated by the slow amplitude changes [17]. Keeping in mind that the target is the estimation of the positive sequence synchrophasor, supposing that the phase quantities have been properly measured with a sampling time T_s, (12) can be rewritten as

$$\bar{x}(nT_s) = \bar{X}_{1,+,S} + \bar{d}(nT_s) \tag{14}$$

with n integer. The vector disturbance $\bar{d}$ has been introduced, which is given by

$$\bar{d}(nT_s) = \sum_{\substack{k=-\infty\\k\neq 1}}^{\infty}\bar{X}_k\,e^{j[k\theta_1(nT_s)-\beta(nT_s)]} + \sum_{\substack{k=-\infty\\k\neq 0}}^{\infty}\bar{X}_{nh,k}\,e^{j[\mathrm{sgn}\,(k)\theta_{nh,|k|}(nT_s)-\beta(nT_s)]}. \tag{15}$$

It is important to recall that, because of the data acquisition system, $\bar{d}$ also includes its noise and quantization error. However, if a proper acquisition is performed, the contribution is low and does not influence the discussion in the following. For this reason, the standard [1] does not consider wideband noise in the tests, but it can be easily taken into account. Thanks to the choice of the reference frame, the rotational speed of the positive sequence synchrophasor is low, being ω_1 close to its rated value ω_0. Having supposed that the angular frequencies of the disturbing components are significantly different from ω_0, the positive sequence synchrophasor can be extracted through proper low-pass filters. A first filtering stage H can be applied to the real and imaginary part of the SV, x_d and x_q. Assuming that $\bar{H}$ represents its frequency response function, reminding that the variations of angular frequency and magnitude are slow with respect to ω_0, the filtered SV $\bar{x}_f$ results

$$\begin{aligned}\bar{x}_f(nT_s) &= \bar{X}_{1,+,S,f}(nT_s) + \bar{d}_f(nT_s)\\ &= \bar{H}[j(\omega_1-\omega_0)]\bar{X}_{1,+,S}\{nT_s - \tau_H[j(\omega_1-\omega_0)]\}\\ &\quad + \bar{d}_f(nT_s)\end{aligned} \tag{16}$$

being τ_H the group delay of the digital filter H, which only depends on $\omega_1 - \omega_0$, and $\bar{d}_f$ the residual disturbance after filtering. The magnitude x_f and phase φ_f of the filtered SV can be obtained. It is extremely important that H reduces $\bar{d}_f$ as much as possible, since it produces a bias in the magnitude of $\bar{x}_f$ which can no longer be removed. On the other hand, the alternating component of the disturbance in the SV magnitude and phase can be further reduced thanks to a second filtering stage

$$\begin{aligned}x_{f,e}(nT_s - \tau_M) &= \sum_{k=0}^{N_M} x_f[(n-k)T_s]\,M(k)\\ \varphi_{f,e}(nT_s - \tau_P) &= \sum_{k=0}^{N_P}\varphi_f[(n-k)T_s]\,P(k).\end{aligned} \tag{17}$$

M and P are linear-phase FIR filters whose orders are N_M and N_P, respectively. Their (constant) group delays are τ_M and τ_P, which can be easily compensated as in (17).

A PMU, other than the synchrophasor, is supposed to measure system frequency as well as ROCOF. According to their definitions, both these quantities can be computed starting

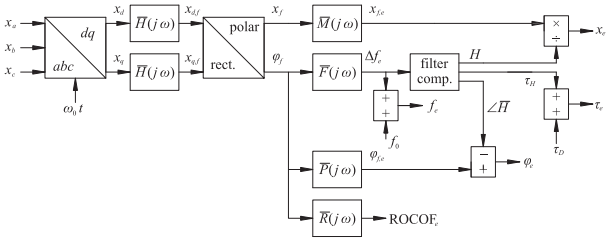

Fig. 1. Block diagram of the proposed PMU algorithm.

from φ_f, the phase of the filtered SV

$$\begin{aligned}\Delta f_e(nT_s - \tau_F) &= \sum_{k=0}^{N_F} \varphi_f[(n-k)T_s]\, F(k) \\ f_e(nTs - \tau_F) &= f_0 + \Delta f_e(nTs - \tau_F) \\ \mathrm{ROCOF}_e(nT_s - \tau_R) &= \sum_{k=0}^{N_R} \varphi_f[(n-k)T_s]\, R(k) \end{aligned} \quad (18)$$

where Δf_e, f_e, and ROCOF_e are, respectively, the frequency deviation, frequency, and ROCOF estimations. Filter F is a properly designed partial-band FIR differentiator, characterized by its order N_F and constant group delay τ_F. Similarly, R is a FIR, N_Rth order, partial-band double differentiator, while τ_R represents its constant group delay.

Even if a stationary, positive sequence input with negligible disturbance is assumed, $x_{f,e}$ and $\varphi_{f,e}$ differ from the actual magnitude and phase of the positive sequence phasor because of the alterations introduced by filtering, in particular by the input filter H. However, from (16), the filter response only depends on the difference between rated and actual angular frequency, hence, on the frequency deviation Δf_e. Therefore, after its estimation, the distortions due to H can be easily compensated. The total group delay τ_e introduced by the algorithm, which is fundamental for time-stamping the estimations, results

$$\begin{aligned}\tau_e &= \tau_H + \tau_D \\ \tau_D &= \max(\tau_M, \tau_P, \tau_F, \tau_R). \end{aligned} \quad (19)$$

Synchrophasor, frequency, and ROCOF are evaluated according to the selected reporting rate. The proposed PMU algorithm based on the SV transformation can be summarized with the block diagram shown in Fig. 1.

IV. Analytical Performance Prediction

The performance of the proposed synchrophasor and frequency estimation technique depends on the frequency response functions $\bar{H}$, $\bar{M}$, $\bar{P}$, $\bar{F}$, and $\bar{R}$ of the filters.[2] This makes the algorithm extremely flexible, since the digital filters can be tailored in order to achieve specific goals according to the peculiar applications. The simple architecture allows to accurately predict the results of P-class and M-class compliance tests specified by the IEEE Standard C37.118.1 [1] through simple analytical expressions.

[2]For the sake of brevity, in the following, H, M, P, F, and R are used to denote the magnitude responses of the filters

A. Steady-State Tests

When considering steady-state tests, the three-phase input signal contains a main, positive sequence component characterized by the positive sequence phasor $\bar{X}_1 = X_1 e^{j\varphi_1}$ and the frequency f_1, or alternatively the angular frequency ω_1. A positive sequence disturbance defined by its positive sequence phasor $\bar{X}_d = X_d e^{j\varphi_d}$ and frequency f_d (angular frequency ω_d) is superimposed. f_d may be multiple of f_1 (harmonic distortion test) or not (out-of-band interference test). An ideal PMU achieves perfect noise rejection, so it returns the frequency f_1, zero ROCOF, and the positive sequence synchrophasor

$$\bar{X}_{1,+,S}(t) = \bar{X}_1 e^{j(\omega_1 - \omega_0)t}. \quad (20)$$

The proposed PMU algorithm first requires to compute the SV of the sampled three-phase signal on the synchronous reference frame whose instantaneous angular position is $\beta = \omega_0 n T_s$

$$\bar{x}(nT_s) = (\bar{X}_1 e^{j\omega_1 nTs} + \bar{X}_d e^{j\omega_d nTs}) e^{-j\omega_0 nTs}. \quad (21)$$

Filter H has to be applied to the direct and quadrature components of $\bar{x}$, thus obtaining $\bar{x}_f$

$$\begin{aligned}\bar{x}_f(nT_s) = {} & [1 + \bar{K} e^{j(\omega_d - \omega_1)nTs}] \\ & \cdot \bar{H}[j(\omega_1 - \omega_0)]\, \bar{X}_1 e^{j(\omega_1 - \omega_0)nTs} \end{aligned} \quad (22)$$

being

$$\bar{K} = K e^{j\varphi_K} = \frac{\bar{H}[j(\omega_d - \omega_0)]}{\bar{H}[j(\omega_1 - \omega_0)]} \frac{\bar{X}_d}{\bar{X}_1}. \quad (23)$$

The amplitude of the disturbance is much lower than the main component and H is a low-pass filter; hence, K is much smaller than one. Under this assumption φ_f, namely, the phase angle of $\bar{x}_f$, can be accurately approximated by a first-order expansion

$$\begin{aligned}\varphi_f(nT_s) = {} & \varphi_1 + \angle \bar{H}[j(\omega_1 - \omega_0)] + (\omega_1 - \omega_0) n T_s \\ & + K \sin[(\omega_d - \omega_1) n T_s + \varphi_k]. \end{aligned} \quad (24)$$

The frequency deviation Δf_e can be evaluated by applying to φ_f the FIR differentiator F. Filters F and H introduce their group delays τ_F and τ_H. The first one is constant, while the second is a function of the frequency deviation itself, hence they can be easily compensated. The gain of filter F has to be set so that its output is 1 Hz for a ramp input signal having a slope of 2π rad/s, thus ensuring a theoretically zero error supposing a constant, off-nominal system frequency and no disturbing components. Being F a linear-phase differentiator, Δf_e is given by

$$\begin{aligned}\Delta f_e(nT_s) = {} & f_1 - f_0 + K \tilde{F}[j(\omega_d - \omega_1)] \\ & \cdot \cos\{(\omega_d - \omega_1)[nT_s + \tau_H(\Delta f_e)] + \varphi_K\} \end{aligned} \quad (25)$$

having introduced $\tilde{F}$ as the amplitude response of filter F. $\mathrm{FE}_{\max}$, namely, the peak value of the FE can be obtained as

$$\mathrm{FE}_{\max} = K F[j(\omega_d - \omega_1)]. \quad (26)$$

The ROCOF is obtained by applying to φ_f the FIR linear phase, double differentiator R. Having compensated the group

delays τ_R and τ_H, having introduced $\tilde{R}$ as the amplitude response of R, the estimated ROCOF can be written as

$$\begin{aligned}\mathrm{ROCOF}_e(nTs) &= K\tilde{R}[j(\omega_d-\omega_1)] \\ &\quad\cdot \sin[(\omega_d-\omega_1)[nT_s+\tau_H(\Delta f_e)]+\varphi_K].\end{aligned} \tag{27}$$

The input signal ROCOF is zero; hence, the peak ROCOF error $\mathrm{RFE}_{\max}$ is

$$\mathrm{RFE}_{\max} = K\,R[j(\omega_d-\omega_1)]. \tag{28}$$

Now, the synchrophasor magnitude and phase have to be assessed. The first can be estimated by applying the low-pass, linear-phase FIR filter M to the SV magnitude. As usual, the group delays can be compensated and $x_{f,e}$ is obtained. If it has unitary dc gain, M does not introduce errors in the case of a purely positive sequence, sinusoidal steady-state input signal. Under these conditions, $x_{f,e}$ is constant but may differ from X_1 if the frequency is not equal to its rated value, because of the magnitude response of the input filter H. Since it depends on the frequency deviation (that has been previously obtained), the resulting error can be compensated, thus leading to the following expression of the estimated synchrophasor magnitude x_e:

$$x_e(nTs) = \{1+KA\cos\{(\omega_d-\omega_1)[nT_s+\tau_H(\Delta f_e)]+\varphi_K\}X_1 \tag{29}$$

where

$$A = \tilde{M}[j(\omega_d-\omega_1)] - \left.\frac{dH(j\omega)}{d\omega}\right|_{\omega=\omega_1-\omega_0}\frac{2\pi\,\tilde{F}[j(\omega_d-\omega_1)]}{H[(j(\omega_1-\omega_0)]}. \tag{30}$$

Being $\tilde{M}$ the amplitude response of filter M. Further details are reported in Appendix A.

The analytical expression of the estimated synchrophasor phase angle can be derived in a similar fashion. The proposed algorithm requires to apply the linear-phase FIR filter P to φ_f. Having compensated the group delays due to filter H and M, $\varphi_{f,e}$ is obtained. If P has unitary dc gain, it does not introduce errors when considering a sinusoidal steady-state, positive sequence input signal. However, input filter H produces a phase shift which biases the estimation of the phase angle. Neglecting the effect of $\bar{X}_d$, this phase shift only depends on the frequency deviation. Therefore, the bias can be removed as for the magnitude estimation. Assuming that H is a linear-phase FIR or a Bessel IIR filter having a cutoff frequency not lower than $|\omega_1-\omega_0|$, it can be written

$$\begin{aligned}\varphi_e(nT_s) &= \varphi_1+(\omega_1-\omega_0)nTs+K\tilde{P}[j(\omega_d-\omega_1)] \\ &\quad\times\sin\{(\omega_d-\omega_1)[nT_s+\tau_H(\Delta f_e)]+\varphi_K\}\end{aligned} \tag{31}$$

where $\tilde{P}$ is the amplitude response of filter P. Since both the magnitude and angle of the synchrophasor have been estimated, it is possible to compute the TVE as defined by the standard. Its expression can be noticeably simplified reminding that K is much lower than one; after some computations omitted for the sake of brevity it results in (32), as shown at the bottom of this page, while its peak value is given by the following compact equation:

$$\mathrm{TVE}_{\max} = K\max\{|A|, P[j(\omega_d-\omega_1)]\}. \tag{33}$$

B. Dynamic Tests

When considering dynamic conditions, the different three-phase test signals suggested in [1] and [2] have to be applied. In the following, the algorithm response to amplitude and phase angle modulations, frequency ramps, and amplitude or phase step signals are discussed in detail, deriving the corresponding estimation errors.

1) Amplitude and Phase Modulation: The generic amplitude and phase modulated three-phase signal is considered as follows:

$$\begin{aligned}x_p(t) &= \sqrt{2}X(1+k_x\cos(\omega_m t)) \\ &\quad\cdot\cos[\omega_0 t+\varphi+\phi_p-k_a\cos(\omega_m t)]\end{aligned} \tag{34}$$

where $p\in\{a,b,c\}$, $\phi_p\in\{0,-(2/3)\pi,(2/3)\pi\}$, and $\omega_m = 2\pi f_m$. f_m is the modulation frequency, while k_x and k_a are the modulation depths for amplitude and phase angle, respectively. From (11), the SV in a nominal frequency reference frame becomes

$$\begin{aligned}\bar{x}(t) &= \frac{1}{\sqrt{3}}X(1+k_x\cos(\omega_m t)) \\ &\quad\cdot[3e^{j[\varphi-k_a\cos(\omega_m t)]} \\ &\qquad + e^{-j[2\omega_0 t+\varphi-k_a\cos(\omega_m t)]}(1+\bar{\alpha}+\bar{\alpha}^2)] \\ &= \bar{X}_1(1+k_x\cos(\omega_m t))e^{-jk_a\cos(\omega_m t)}\end{aligned} \tag{35}$$

where the last equality is obtained by recognizing that $1+\bar{\alpha}+\bar{\alpha}^2=0$, and thus, the $2\omega_0$ terms are canceled, while $\bar{X}_1 = \sqrt{3}Xe^{j\varphi}$. An ideal PMU returns exactly the positive sequence synchrophasor $\bar{X}_{1,+,S}$ that is equal to the SV $\bar{x}$. Furthermore, an ideal PMU would estimate frequency f and ROCOF with zero errors, hence

$$\begin{aligned}f(t) &= f_0+k_a\frac{\omega_m}{2\pi}\sin(\omega_m t) \\ \mathrm{ROCOF}(t) &= k_a\frac{\omega_m^2}{2\pi}\cos(\omega_m t).\end{aligned} \tag{36}$$

In the following, formulas for the maximum errors in the specific test cases are reported.

a) Amplitude modulation: First, the amplitude modulation ($k_a = 0$) is considered. After sampling the phase quantities, the filtered SV results

$$\bar{x}_f(nT_s) = \bar{X}_1[1+k_x H(j\omega_m)\cos(\omega_m t+\angle\bar{H}(j\omega_m))] \tag{37}$$

$$\mathrm{TVE}(nT_s) = \frac{K}{\sqrt{2}}\sqrt{A^2+P^2[j(\omega_d-\omega_1)]+\{A^2-P^2[j(\omega_d-\omega_1)]\}\cos\{[2(\omega_d-\omega_1)[nT_s+\tau_H(\Delta f_e)]+2\varphi_K\}} \tag{32}$$

where it is clear that the phase angle of $\bar{x}_f(t)$ is $\varphi_f(t) = \varphi$. As aforementioned, the frequency is estimated by means of the FIR filter F, thus resulting in a computed frequency deviation $\Delta f_e = F(j0)\varphi = 0$, since the derivator filter has zero dc amplitude. For this reason, the maximum FE is $\mathrm{FE}_{\max} = 0$. The same consideration holds for ROCOF ($\mathrm{RFE}_{\max} = 0$).

The phasor amplitude estimation leads to the following expression (assuming $M(j0) = 1$, and using the amplitude responses $\tilde{M}$ and $\tilde{H}$ of filter M and H, respectively):

$$x_e(nT_s) = X_1(1 + k_x \tilde{M}(j\omega_m)\tilde{H}(j\omega_m)\cos(\omega_m n T_s + \alpha_{HM})) \tag{38}$$

being

$$\alpha_{HM} = \omega_m \tau_H(0) + \angle\left(\frac{\bar{H}(j\omega_m)}{\tilde{H}(j\omega_m)}\right). \tag{39}$$

Scalloping loss due to filter H has now to be compensated; since a zero frequency deviation has been measured, it results in a correction factor $H(j0) = 1$ which does not affect the estimation.

Phase estimation is very simple being $\varphi_f = \varphi$. The FIR filtering (for instance, the LSs estimation) leads to an unbiased phase estimation, assuming unitary dc gain of P. From these assumptions, the maximum TVE of the estimated synchrophasor can be derived (see Appendix B for details) as follows:

$$\mathrm{TVE}_{\max} = \frac{[1 + \tilde{M}(j\omega_m)\tilde{H}(j\omega_m)]}{\frac{1}{|k_x|} - 1}. \tag{40}$$

b) Phase modulation: With a similar approach, the maximum TVE expression can be derived for the phase modulation test. In this case, the digitally filtered SV signal becomes [$H(j0) = 1$ still supposed]

$$\begin{aligned}\bar{x}_f(nT_s) &= \bar{X}_1(1 - jk_a H(j\omega_m)\cos(\omega_m t + \angle\bar{H}(j\omega_m))) \\ &\simeq \bar{X}_1 e^{-jk_a H(j\omega_m)\cos(\omega_m t + \angle\bar{H}(j\omega_m))}\end{aligned} \tag{41}$$

where the approximation holds for small modulation depths. Phase and frequency can be obtained by means of filter P and F. It is possible to show that (see Appendix B for details) the maximum FE, when H is a symmetrical FIR or Bessel filter, results

$$\mathrm{FE}_{\max} = |k_a f_m| \left|1 - \frac{\tilde{F}(j\omega_m)}{f_m}\tilde{H}(j\omega_m)\right|. \tag{42}$$

Analogously, the derivation of ROCOF can be obtained considering the double differentiator R. The maximum error becomes

$$\mathrm{RFE}_{\max} = \left|2\pi k_a f_m^2\right| \left|1 - \frac{\tilde{R}(j\omega_m)}{2\pi f_m^2}\tilde{H}(j\omega_m)\right|. \tag{43}$$

Besides, after a few passages reported in Appendix B, an approximate expression for the maximum TVE can be obtained as follows:

$$\mathrm{TVE}_{\max} \simeq |k_a||1 - \tilde{H}(j\omega_m)\tilde{P}(j\omega_m)| \tag{44}$$

thus corresponding, approximately, to the attenuation of the phase filter chain at the modulation frequency.

2) Input Step Change Tests: Input step change tests require to apply a three-phase balanced signal at the rated frequency which contains a step change in either amplitude or phase. Supposing that the step occurs in $t = 0$, an ideal PMU should return exactly the frequency f_0, zero ROCOF and an estimated positive sequence synchrophasor given by

$$\bar{X}_{1,+,S}(t) = \bar{X}_1[1 + k_x\, u(t)]e^{jk_a u(t)} \tag{45}$$

being $u(t)$ the unity step function, k_x and k_a the amplitude and phase jump step size, respectively.

a) Amplitude step change test: First of all, let us consider the amplitude step change test, which corresponds to $k_x \neq 0$ and $k_a = 0$ in (45). As usual, the proposed algorithm requires to sample the waveforms and compute the SV on the synchronous reference frame

$$\bar{x}(nT_s) = \bar{X}_1[1 + k_x\, u(nT_s)]. \tag{46}$$

Then, filter H has to be applied to the real and imaginary parts of $\bar{x}$, thus obtaining $\bar{x}_f$. Introducing h as its unit step response

$$\bar{x}_f(nT_s) = \bar{X}_1[1 + k_x\, h(nT_s)]. \tag{47}$$

The phase angle of the filtered SV is constant. Therefore, the proposed algorithm returns zero frequency deviation and ROCOF, thus leading to zero FE and RFE in this test.

The magnitude of the synchrophasor is estimated by applying the FIR filter M. Let us introduce mh as the unit step response of the cascade of filters M and H. Since H (other than M) has unity dc gain and the estimated frequency deviation is zero, the compensation of its frequency response has no effect. However, the group delays introduced by the filters have to be taken into account, therefore

$$\bar{x}_e(nT_s) = \bar{X}_1[1 + k_x\, mh(nT_s + \tau_H(0) + \tau_M)]. \tag{48}$$

The synchrophasor phase angle is computed by applying the FIR filter P to the phase of $\bar{x}_f$. Since this phase angle is constant, P has unity dc gain and the estimated frequency deviation is zero, $\varphi_f = \varphi$.

From the magnitude and phase estimations of the positive sequence synchrophasor, the TVE can be computed as

$$\begin{cases}\mathrm{TVE}(nT_s) = |k_x\, mh(nT_s + \tau_H(0) + \tau_M)| & n < 0 \\ \mathrm{TVE}(nT_s) = \dfrac{|k_x|}{1 + k_x}\,|mh(nT_s + \tau_H(0) + \tau_M) - 1| & n > 0.\end{cases} \tag{49}$$

b) Phase step change test: The same procedure will be applied to the phase step change test; hence, $k_a \neq 0$ and $k_x = 0$. In this case, sampling the time-domain waveforms and computing the SV on the rotating reference frame lead to

$$\bar{x}(nT_s) = \bar{X}_1 e^{jk_a u(nT_s)} \simeq \bar{X}_1[1 + jk_a\, u(nT_s)] \tag{50}$$

being $k_a \ll 1$. First of all, the low-pass filter H has to be applied to the real and imaginary part of $\bar{x}$, thus obtaining $\bar{x}_f$

$$\bar{x}_f(nT_s) = \bar{X}_1[1 + jk_a\, h(nT_s)] \simeq \bar{X}_1 e^{jk_a h(nT_s)}. \tag{51}$$

As usual, the frequency is estimated by applying the FIR differentiator F to the phase angle of $\bar{x}_f$. Introducing fh as the unit step response of the cascade between filter F and H

and compensating the group delays, the estimated frequency results

$$\begin{aligned} f_e(nT_s) &= f_0 + \Delta f_e(nT_s) \\ &= f_0 + k_a\ fh(nT_s + \tau_H(0) + \tau_F). \end{aligned} \tag{52}$$

The effect of the estimated frequency on the group delay compensation has been neglected: it is extremely small since H is a symmetrical FIR or Bessel IIR filter. Hence, the FE can be easily computed as

$$\mathrm{FE}(nT_s) = |k_a\ fh(nT_s + \tau_H(0) + \tau_F)|. \tag{53}$$

In a similar fashion, ROCOF is computed from the phase of $\bar{x}_f$ by applying the FIR double differentiator R. Being rh the unit step response of the cascade of filter H and R, having compensating the group delays, the ROCOF estimation is given by

$$\mathrm{ROCOF}_e(nT_s) = k_a\ rh(nT_s + \tau_H(0) + \tau_R). \tag{54}$$

and the corresponding RFE

$$\mathrm{RFE}(nT_s) = |k_a\ rh(nT_s + \tau_H(0) + \tau_R)|. \tag{55}$$

The magnitude of the positive sequence synchrophasor is estimated by taking the magnitude of $\bar{x}_f$, applying filter M, and compensating the effect of filter H. Since x_f is constant while $M(j0) = 1$ and $H(j0) = 1$, it can be written

$$x_e = \frac{X_1}{H(j2\pi\,\Delta f_e)} \simeq X_1 \tag{56}$$

having noticed that the estimated frequency deviation is very small and that the magnitude response of H has nil derivative near zero.

After that, the phase of the positive sequence synchrophasor has to be assessed. It is obtained by applying filter P to the phase of $\bar{x}_f$. Defining ph as the unit step response of the cascade between filter H and P and compensating the group delays, the estimated phase angle φ_e results

$$\varphi_e(nT_s) = k_a\ ph(nT_s + \tau_H(0) + \tau_P). \tag{57}$$

As for the magnitude estimation, compensating the phase shift introduced by H has a negligible impact on phase angle estimation, since the evaluated frequency deviation is very small and H is exactly or almost linear phase in the passband.

The estimated synchrophasor can be computed and the TVE is obtained

$$\begin{cases} \mathrm{TVE}(nT_s) = |e^{jk_a\ ph(nT_s - \tau_H(0) - \tau_P)} - 1| \\ \qquad\qquad \simeq |k_a\ ph(nT_s - \tau_H(0) - \tau_P)| \qquad n < 0 \\ \mathrm{TVE}(nT_s) = |e^{jk_a\ ph(nT_s - \tau_H(0) - \tau_P)} - e^{jk_a}| \\ \qquad\qquad \simeq |k_a|\,|ph(nT_s - \tau_H(0) - \tau_P) - 1| \quad n > 0. \end{cases} \tag{58}$$

3) Frequency Ramp Test: Considering the frequency ramp test, the sampled SV signal can be represented with respect to the ramp initial instant as

$$\bar{x}(nT_s) = \bar{X}_1 e^{j\pi R_f (nT_s)^2} \tag{59}$$

where R_f is the constant ROCOF value. When considering a generic PMU measurement instant $t_r = n_r T_s$ during the ramp, (59) can be easily written considering the angular speed $\Delta\omega_r = 2\pi R_f t_r = \omega_r - \omega_0$. The filtered signal at the first stage thus depends on $\bar{H}(j2\pi R_f t_r)$ and it is possible to show that the phase is $\varphi_f(nT_s) \simeq \varphi_r + R_f t_r (nT_s - t_r) + \angle\bar{H}(j\omega_r)$. For this reason, both the frequency and the ROCOF estimations lead to the exact values if the coefficients of F and R are normalized so that they give as outputs $R_f t_r$ and R_f, respectively. With this assumption, the amplitude compensation at each measurement point follows straightforwardly, while phase compensation depends on $\angle\bar{H}(j\omega_r)$ and the group delay compensation is performed as previously discussed for the other test conditions.

V. Filter Design

The expressions reported in Section IV allow predicting the measurement performance of the proposed PMU algorithms starting from the frequency response functions and unit step responses of the digital filters H, M, P, F, and R. This permits a quick adjustment of said filters in order to meet the user's requirements, as, for example, those indicated by specific performance goals for the tests suggested by [1] and [2].

The input filter H is extremely critical: its task is to remove most part of the disturbances, thus has a significant impact on all the performance tests. As stated earlier, H can be a linear-phase FIR but also a Bessel IIR low-pass filter, characterized by a step response without overshoot or ringing and an almost linear phase within its passband. The latter choice permits to reduce the computational burden of the algorithm as in [17], even if the best performance is achieved by using a symmetrical FIR filter, as in this paper.

It should also be noticed that, under the assumptions introduced earlier, for most of the tests, the limits in terms of maximum TVE, FE, or RFE can be translated into constraints about the amplitude responses of the filters. Hence, in order to comply with these limits, the low-pass, symmetrical FIR filters H, M, and P can be designed by using the equiripple method, thus specifying passband and stopband frequencies and magnitudes. Their coefficients have to be normalized in order to have unitary dc gain, which permits to achieve a theoretically zero error under stationary conditions.

Filters F and R are key to achieve remarkable performances in terms of FE and RFE during the harmonic distortion and out-of-band interference tests, which are notoriously the most severe ones. They have been designed as band-limited, linear-phase FIR differentiators by specifying the stopband frequency and a very high stopband weight coefficient in order to increase attenuation above passband. The coefficients of filter F have to be scaled so that its output is unitary when the input signal phase angle is a ramp having a slope of 2π rad/s,

TABLE I

EXAMPLE OF FILTER PARAMETERS FOR THE DESIGN OF A P-CLASS PMU

Filter	**Passband Frequency [Hz]**	**Stopband Frequency [Hz]**	**Passband Ripple** (linear units)	**Stopband Ripple** (linear units)
H	2	50	2e-3	0.03
M	2	50	0.01	0.03
P	2	50	0.01	0.03
Filter	**Passband Frequency [Hz]**	**Stopband Frequency [Hz]**	**Filter Order**	**Stopband Weight** (linear units)
F	2	50	36	100
R	2	50	36	1000

which ensures a theoretically zero FE in off-nominal system frequency conditions. Similarly, the coefficients of filter R should be normalized in order to obtain a unitary output with a parabolic input signal having an amplitude of π rad/s^2. In this way, the steady-state RFE is theoretically zero during a frequency ramp.

Satisfying the constraints about the amplitude responses of the filters allows compliance with the limits indicated by [2] for steady-state and modulation tests. Usually, also the frequency ramp test can be easily passed. However, the latency of the algorithm has to be checked: it can be easily obtained from the group delays of the filters, leaving an adequate margin for computation. Finally, the results of the input step change tests can be predicted by using the analytical formulas based on the step responses of the filters and compared with the limits.

VI. TEST RESULTS

In the following, examples of filter design parameters which allow the algorithm to comply with M and P performance classes are reported, together with the test results obtained according to the standard. Since [2] does not specify the maximum values of RFE for the harmonic distortion and out-of-band interference tests, the limits reported in [1] have been considered here. A sampling rate as low as 800 Hz has been selected (as in [1, Annex C]); it allows reducing the number of filter taps and hence the computational burden. However, an adequate antialiasing filter is required; alternatively, the electrical quantities can be sampled with a much higher rate, and then decimated after digital filtering. This choice allows avoiding the accuracy degradation due to the drift of passive components. In any case, a proper design of these filters does not significantly affect the performance achieved by the proposed algorithm. The results refer to a reporting rate $F_s = 50$ phasors/s, which is the highest mandatory value set by the standard for PMUs operating in 50-Hz systems.

The P-class PMU example is considered at first; the filter design parameters reported in Table I have been employed. This choice allows in a simple way the compliance with the requirements of [2], as summarized by Table II. For each test result, the maximum value for the testing conditions and, between parentheses, the corresponding limit found with the analytic expressions illustrated in Section IV are reported. Between brackets, the limit requested by the standard is always

TABLE II

ACCURACY RESULTS FOR THE DESIGNED P-CLASS PMU. ANALYTICAL PREDICTIONS REPORTED IN ROUND BRACKETS, LIMITS IN SQUARE BRACKETS

Test	**TVE [%]**	**FE [mHz]**	**RFE [Hz/s]**
Off-nominal $[48-52]$ Hz	~ 0 [1] (0)	~ 0 [5] (0)	~ 0 [0.4] (0)
Harmonics [2nd harm.]	$6.74 \cdot 10^{-4}$ [1] $(6.72 \cdot 10^{-4})$	$4.27 \cdot 10^{-2}$ [5] $(4.27 \cdot 10^{-2})$	0.0532 [0.4] (0.0532)
Amplitude modulation	0.077 [3] (0.077)	0 [60] (0)	~ 0 [2.3] (0)
Phase modulation	0.069 [3] (0.069)	1.74 [60] (1.74)	0.021 [2.3] (0.021)
Frequency ramp	0.028 [1] $(-)$	$9.8 \cdot 10^{-5}$ [10] $(-)$	~ 0 [0.4] $(-)$

Step test	**response time [ms]**			**delay time [ms]**	**over/undershoot [%]**
	t_{TVE}[a]	t_{FE}[b]	t_{RFE}[c]		
Amplitude step	27.5 [40] (27.5)	0 [90] (0)	0 [120] (0)	~ 0 [5] (0)	0 [5] (0)
Phase step	32.5 [40] (32.5)	67.5 [90] (67.5)	72.5 [120] (72.5)	~ 0 [5] (0)	~ 0 [5] (0)

[a] the time during which TVE is outside the steady-state limit.
[b] the time during which FE is outside the steady-state limit.
[c] the time during which RFE is outside the steady-state limit.

TABLE III

EXAMPLE OF FILTER PARAMETERS FOR THE DESIGN OF A M-CLASS PMU

Filter	**Passband Frequency [Hz]**	**Stopband Frequency [Hz]**	**Passband Ripple** (linear units)	**Stopband Ripple** (linear units)
H	5	25	2e-3	0.03
M	5	25	0.01	0.01
P	5	25	0.01	0.01
Filter	**Passband Frequency [Hz]**	**Stopband Frequency [Hz]**	**Filter Order**	**Stopband Weight** (linear units)
F	5	25	128	100
R	5	25	128	1000

indicated as a reference. It is clear that the predictions of the analytical formulas are extremely close to the test results, which in turn are far below the limits. Results confirm that thanks, above all, to the design of filter H and its compensation at the estimated frequency, the errors are almost zero in off-nominal frequency conditions. Harmonic disturbances are strongly attenuated by the cascade of filters: for instance, FE is reduced due to the contributions of H and F stop-bands. The theoretical PMU latency, due to the filter length, is 36.2 ms.

As for the M-class PMU design, a similar strategy can be adopted and the filter parameters reported in Table III have been considered. Also in this case, the predicted maximum TVE, FE, and RFE are very close to those achieved during the tests, and they are far below the required limits for the maximum reporting rate of 50 phasors/s, as shown in Table IV (which uses the same notation as Table II for the

TABLE IV

ACCURACY RESULTS FOR THE DESIGNED M-CLASS PMU. ANALYTICAL PREDICTIONS REPORTED IN ROUND BRACKETS, LIMITS IN SQUARE BRACKETS

Test	**TVE [%]**			**FE [mHz]**	**RFE [Hz/s]**
Off-nominal $[45-55]$ Hz	~ 0 [1] (0)			~ 0 [5] (0)	~ 0 [0.1] (0)
Harmonics [2nd harm.]	$2.22 \cdot 10^{-3}$ [1] $(2.06 \cdot 10^{-3})$			$1.1 \cdot 10^{-2}$ [25] $(1.1 \cdot 10^{-2})$	$4.6 \cdot 10^{-4}$ [6] $(4.6 \cdot 10^{-4})$
Out-of-band interference	$2.16 \cdot 10^{-2}$ [1.3] $(2.14 \cdot 10^{-2})$			1.41 [10] (1.41)	0.0153 [0.1] (0.0154)
Amplitude modulation	0.249 [3] (0.249)			0 [300] (0)	~ 0 [14] (0)
Phase modulation	0.225 [3] (0.224)			2.13 [300] (2.16)	3.32 [14] (3.32)
Frequency ramp	0.030[1] (−)			$1.5 \cdot 10^{-2}$[10] (−)	~ 0 [0.2] (−)
Step test	**response time [ms]**			**delay time [ms]**	**over/undershoot [%]**
	t_{TVE}	t_{FE}	t_{RFE}		
Amplitude step	37.5 [140] (37.5)	0 [280] (0)	0 [280] (0)	0 [5] (0)	4.34 [10] (4.34)
Phase step	42.5 [140] (42.5)	120 [280] (120)	174 [280] (174)	0 [5] (0)	4.33 [10] (4.34)

limits and analytical predictions). The main difference with respect to P-class design is due to the out-of-band interference test: in this case, disturbance rejection requires filters having a significant attenuation from half of the reporting rate (as reported in Table III) which unavoidably results in a narrower passband. The theoretical latency is 124 ms, as defined by filter lengths, with respect to a limit equal to 140 ms.

The reported examples are intended to show the high level of flexibility allowed by the proposed approach in PMU design. As aforementioned, the standard [1, Annex C], suggests to use a demodulation and filtering approach for both P and M classes. In that case, a single filter is used for disturbance rejection while frequency and ROCOF are obtained by discrete derivatives of the estimated phase angle. For this reason, the performance in terms of FE and RFE relies only on the filter stopband and passband behavior. Focusing on the suggested M-class filter (sample rate is the same as in the proposed implementation, 800 Hz, and $F_s = 50$ phasors/s), it achieves higher TVE values with respect to Table IV under off-nominal (0.113%) and frequency ramp conditions (0.088%), while FE and, above all, RFE are considerably larger in presence of harmonics (max RFE = 8.3 Hz/s, for harmonic order $k = 7$) and interharmonics (max RFE = 2.0 Hz/s, for example, when the interharmonic frequency is 98 Hz). These results strongly depend on the specific filter design, but they show how the proposed approach allows more degrees of freedom, for instance, in frequency and ROCOF estimation. In the M-class design example, the stopbands of the differentiators allowed achieving high rejection of out-of-band interferences, but the flexible architecture based on five filters permits to tailor the phasor, frequency, and ROCOF measurement performance separately, in order to cope with specific requirements.

VII. CONCLUSION

This paper proposes a flexible approach for synchrophasor, frequency, and ROCOF estimation which exploits the SV transformation and digital filters. The computations are performed in time domain, thus avoiding spectral leakage effects which are typical of DFT-based techniques under off-nominal frequency conditions. Since the algorithm is conceptually extremely simple, its performance in terms of TVE, FE, RFE, and step response can be predicted by means of simple analytical expressions, starting from the filter coefficients. From another point of view, these expressions allow an effective filter design in order to suit specific accuracy targets. As examples, the proposed approach has been employed to design two PMU algorithms which are able to meet all M-class and P-class requirements with ample margin. Performance predicted by using the analytical expressions results to be extremely close to that obtained by simulation.

APPENDIX A
MAGNITUDE ESTIMATION FOR STEADY-STATE TESTS

Let us start from the magnitude of the filtered SV; (22) can be written as

$$x_f(nT_s) = d(nT_s)\, H[j(\omega_1 - \omega_0)]X_1. \tag{A.1}$$

Being K much smaller than one, the expression of d can be linearized in K

$$d(nT_s) = 1 + K\, \cos[(\omega_d - \omega_1)nT_s + \varphi_K]. \tag{A.2}$$

The magnitude of the filtered SV can be obtained by applying filter M to x_f. The group delays of filter M and H have to be compensated, as well as the magnitude response of filter H which only depends on the frequency deviation. In this way, the estimated synchrophasor magnitude x_e is obtained as

$$\begin{aligned} x_e(nTs) = \{1 &+ K\tilde{M}[j(\omega_d - \omega_1)] \\ &\cdot \cos[(\omega_d - \omega_1)(nT_s + \tau_H(\Delta f_e)) + \varphi_K]\} \\ &\cdot \frac{H[j(\omega_1 - \omega_0)]}{H(j2\pi\,\Delta f_e)} X_1. \end{aligned} \tag{A.3}$$

From (25), the frequency deviation contains an oscillating component due to the disturbance; therefore, also $H(j2\pi\,\Delta f_e)$ contains an alternating term. Since this oscillation is small, a first-order expansion can be employed. This leads to

$$\begin{aligned} H(j2\pi\,\Delta f_e) = H[(j(\omega_1 - \omega_0)] &+ 2\pi\, \left.\frac{dH(j\omega)}{d\omega}\right|_{\omega=\omega_1-\omega_0} \\ &\cdot K\tilde{F}[(j\omega_d - \omega_1)] \\ &\cdot \cos\{(\omega_d - \omega_1)[nT_s + \tau_H(\Delta f_e)] + \varphi_K\}. \end{aligned} \tag{A.4}$$

Substituting (A.4) in (29), while reminding that the oscillating part of $H(j2\pi\,\Delta f_e)$ is small, permits to obtain the analytical expression (29) of the estimated synchrophasor magnitude.

APPENDIX B
TVE AND FE FOR MODULATION TESTS

A. Amplitude Modulation

From the amplitude (38) and phase estimations, TVE can be written as

$$\begin{aligned}\mathrm{TVE}(nT_s) = &\frac{|k_x|}{1+k_x\cos(\omega_m nT_s)}\\ &\cdot|(1-\tilde{M}(j\omega_m)\tilde{H}(j\omega_m)\cos\alpha_{HM})\cos(\omega_m nT_s)\\ &+\tilde{M}(j\omega_m)\tilde{H}(j\omega_m)\sin\alpha_{HM}\sin(\omega_m nT_s)|\end{aligned} \tag{B.1}$$

and defining

$$\begin{aligned}\theta_M \triangleq \arctan 2(&\tilde{M}(j\omega_m)\tilde{H}(j\omega_m)\sin\alpha_{HM},\\ &1-\tilde{M}(j\omega_m)\tilde{H}(j\omega_m)\cos\alpha_{HM})\end{aligned} \tag{B.2}$$

the expression becomes

$$\begin{aligned}\mathrm{TVE}(nT_s) = &\frac{|k_x\cos(\omega_m nT_s-\theta_M)|}{1+k_x\cos(\omega_m nT_s)}\\ &\cdot\sqrt{1+[M(j\omega_m)H(j\omega_m)]^2-2\tilde{M}(j\omega_m)\tilde{H}(j\omega_m)\cos\alpha_{HM}}.\end{aligned} \tag{B.3}$$

From (B.3), it is simple to derive the maximum TVE expression (40).

B. Phase Modulation

From (41), phase and frequency can be obtained by means of $\bar{P}$ and $\bar{F}$ filters. The frequency estimation thus results in

$$\begin{aligned}&\Delta f_e(nT_s-\tau_F-\tau_H(\Delta f_{e,f}))\\ &\quad=-k_a F(j\omega_m)H(j\omega_m)\\ &\qquad\cdot\cos(\omega_m nT_s+\angle\bar{H}(j\omega_m)+\angle\bar{F}(j\omega_m))\end{aligned} \tag{B.4}$$

where group delay compensation has been performed. Reminding that F is a linear phase, band-limited differentiator, it follows:

$$\Delta f_e(nT_s) = k_a\tilde{F}(j\omega_m)\tilde{H}(j\omega_m)\sin(\omega_m nT_s+\alpha_{HP}) \tag{B.5}$$

where $\alpha_{HP}=\omega_m\tau_H(\Delta f_e)+\angle(\bar{H}(j\omega_m)/\tilde{H}(j\omega_m))$. From such expressions, the FE is easily computed

$$\begin{aligned}\mathrm{FE}(nT_s) = |k_a f_m|\cdot\Bigg|&\sin(\omega_m nT_s)-\frac{\tilde{F}(j\omega_m)}{f_m}\tilde{H}(j\omega_m)\\ &\cdot\sin(\omega_m nT_s+\alpha_{HP})\Bigg|\end{aligned} \tag{B.6}$$

and, after a few passages, it follows:

$$\begin{aligned}\mathrm{FE}(nT_s) = &|k_a f_m|\cdot\cos(\omega_m nT_s+\theta_P)\\ &\cdot\sqrt{1+\left[\frac{\tilde{F}(j\omega_m)}{f_m}\tilde{H}(j\omega_m)\right]^2-2\frac{\tilde{F}(j\omega_m)}{f_m}H(j\omega_m)\cos\alpha_{HP}}\end{aligned} \tag{B.7}$$

where

$$\begin{aligned}\theta_F \triangleq \arctan 2\Bigg(&1-\left[\frac{F(j\omega_m)}{f_m}H(j\omega_m)\cos\alpha_{HP}\right],\\ &\frac{F(j\omega_m)}{f_m}H(j\omega_m)\sin\alpha_{HP}\Bigg).\end{aligned} \tag{B.8}$$

From (B.7), it is easy to derive the maximum FE

$$\begin{aligned}\mathrm{FE}_{\max} = &|k_a f_m|\\ &\cdot\sqrt{1+\left[\frac{\tilde{F}(j\omega_m)}{f_m}\tilde{H}(j\omega_m)\right]^2-2\frac{\tilde{F}(j\omega_m)}{f_m}\tilde{H}(j\omega_m)\cos\alpha_{HP}}\end{aligned} \tag{B.9}$$

and considering a symmetrical FIR filter or a Bessel filter for $\bar{H}$, (B.9) reduces to (42).

From the filtered SV (41), it is clear that $x_f = X_1$, that is unaltered when filtered by M. However, the amplitude compensation for filter H leads to $x_e(nT_s) = (X_1/(H(j2\pi\,\Delta f_e)))$. Considering the expression of estimated frequency deviation in (B.5), the estimated amplitude is

$$\begin{aligned}x_e(nT_s) \simeq X_1\Bigg(1-&\left.\frac{dH(j\omega)}{d\omega}\right|_{\omega=0}2\pi\,k_a\tilde{F}(j\omega_m)\tilde{H}(j\omega_m)\\ &\cdot\sin(\omega_m nT_s+\alpha_{HP})\Bigg)\end{aligned} \tag{B.10}$$

where H is approximated with its first-order Maclaurin expansion.

Starting again from (41) and filtering the phase angle by P, it is possible to obtain the realigned phase estimation

$$\begin{aligned}\varphi_e(nT_s) = \varphi-k_a\tilde{H}(j\omega_m)\tilde{P}(j\omega_m)\cos(\omega_m nT_s+\alpha_{HP})+\\ -\angle\bar{H}(j2\pi\,\Delta f_e)-2\pi\,\Delta f_e\tau_H(\Delta f_e).\end{aligned} \tag{B.11}$$

If the filter delay for $\bar{H}$ can be considered constant in the passband, and thus, $\tau_H(\Delta f_e) = -\left.\frac{d\angle\bar{H}}{d\omega}\right|_{\omega=0}$

$$\varphi_e(nT_s) = \varphi-k_a\tilde{H}(j\omega_m)\tilde{P}(j\omega_m)\cos(\omega_m nT_s+\alpha_{HP}). \tag{B.12}$$

The estimated TVE can be calculated from (B.10) and (B.12)

$$\begin{aligned}\mathrm{TVE}(nT_s) = \Bigg|&\Bigg(1-\left.\frac{dH(j\omega)}{d\omega}\right|_{\omega=0}2\pi\,k_a\tilde{F}(j\omega_m)\tilde{H}(j\omega_m)\\ &\cdot\sin(\omega_m nT_s+\alpha_{HP})\Bigg)\\ &\cdot e^{-jk_a\tilde{H}(j\omega_m)\tilde{P}(j\omega_m)\cos(\omega_m nT_s+\alpha_{HP})}\\ &-e^{-jk_a\cos(\omega_m nT_s)}\Bigg|.\end{aligned} \tag{B.13}$$

With the aforementioned assumptions on H, $\alpha_{HP}\simeq 0$; hence, the maximum TVE becomes (B.14), as shown at the bottom of this page page, that can be approximated as in (44).

$$\mathrm{TVE}_{\max}\simeq|k_a|\cdot\sqrt{\left[\left.\frac{dH(j\omega)}{d\omega}\right|_{\omega=0}2\pi\,\tilde{F}(j\omega_m)\tilde{H}(j\omega_m)\right]^2+[1-\tilde{H}(j\omega_m)\tilde{P}(j\omega_m)]^2} \tag{B.14}$$

REFERENCES

[1] *IEEE Standard for Synchrophasor Measurements for Power Systems*, IEEE Standard C37.118.1-2011 (Revision of IEEE Standard C37.118-2005), Dec. 2011.

[2] *IEEE Standard for Synchrophasor Measurements for Power Systems—Amendment 1: Modification of Selected Performance Requirements*, IEEE Standard C37.118.1a-2014 (Amendment to IEEE Standard C37.118.1-2011), Apr. 2014.

[3] M. Karimi-Ghartemani, B.-T. Ooi, and A. Bakhshai, "Application of enhanced phase-locked loop system to the computation of synchrophasors," *IEEE Trans. Power Del.*, vol. 26, no. 1, pp. 22–32, Jan. 2011.

[4] J. A. de la O Serna, "Dynamic phasor estimates for power system oscillations," *IEEE Trans. Instrum. Meas.*, vol. 56, no. 5, pp. 1648–1657, Oct. 2007.

[5] M. A. Platas-Garza and J. A. de la O Serna, "Dynamic phasor and frequency estimates through maximally flat differentiators," *IEEE Trans. Instrum. Meas.*, vol. 59, no. 7, pp. 1803–1811, Jul. 2010.

[6] P. Castello, J. Liu, A. Monti, C. Muscas, P. A. Pegoraro, and F. Ponci, "Toward a class 'P + M' phasor measurement unit," in *Proc. IEEE Int. Workshop Appl. Meas. Power Syst. (AMPS)*, Sep. 2013, pp. 91–96.

[7] P. Castello, J. Liu, C. Muscas, P. A. Pegoraro, F. Ponci, and A. Monti, "A fast and accurate PMU algorithm for P+M class measurement of synchrophasor and frequency," *IEEE Trans. Instrum. Meas.*, vol. 63, no. 12, pp. 2837–2845, Dec. 2014.

[8] P. Romano and M. Paolone, "Enhanced interpolated-DFT for synchrophasor estimation in FPGAs: Theory, implementation, and validation of a PMU prototype," *IEEE Trans. Instrum. Meas.*, vol. 63, no. 12, pp. 2824–2836, Dec. 2014.

[9] D. Petri, D. Fontanelli, and D. Macii, "A frequency-domain algorithm for dynamic synchrophasor and frequency estimation," *IEEE Trans. Instrum. Meas.*, vol. 63, no. 10, pp. 2330–2340, Oct. 2014.

[10] A. J. Roscoe, "Exploring the relative performance of frequency-tracking and fixed-filter phasor measurement unit algorithms under C37.118 test procedures, the effects of interharmonics, and initial attempts at merging p-class response with m-class filtering," *IEEE Trans. Instrum. Meas.*, vol. 62, no. 8, pp. 2140–2153, Aug. 2013.

[11] J. A. de la O Serna and J. Rodriguez-Maldonado, "Instantaneous oscillating phasor estimates with Taylor^K–Kalman filters," *IEEE Trans. Power Syst.*, vol. 26, no. 4, pp. 2336–2344, Nov. 2011.

[12] J. Liu, F. Ni, P. A. Pegoraro, F. Ponci, A. Monti, and C. Muscas, "Fundamental and harmonic synchrophasors estimation using modified Taylor–Kalman filter," in *Proc. IEEE Int. Workshop Appl. Meas. Power Syst. (AMPS)*, Sep. 2012, pp. 1–6.

[13] M. Bertocco, G. Frigo, C. Narduzzi, C. Muscas, and P. A. Pegoraro, "Compressive sensing of a Taylor–Fourier multifrequency model for synchrophasor estimation," *IEEE Trans. Instrum. Meas.*, vol. 64, no. 12, pp. 3274–3283, Dec. 2015.

[14] C. Muscas and P. A. Pegoraro, "Algorithms for synchrophasors, frequency, and ROCOF," in *Phasor Measurement Units and Wide Area Monitoring Systems*, A. Monti, C. Muscas, and F. Ponci, Eds., 1st ed. San Diego, CA, USA: Academic, 2016, ch. 3, pp. 21–51.

[15] D. Macii, G. Barchi, and D. Petri, "Design criteria of digital filters for synchrophasor estimation," in *Proc. IEEE Int. Instrum. Meas. Technol. Conf. (IMTC)*, May 2013, pp. 1579–1584.

[16] A. J. Roscoe, B. Dickerson, and K. E. Martin, "Filter design masks for C37.118.1a-compliant frequency-tracking and fixed-filter m-class phasor measurement units," *IEEE Trans. Instrum. Meas.*, vol. 64, no. 8, pp. 2096–2107, Aug. 2015.

[17] S. Toscani and C. Muscas, "A space vector based approach for synchrophasor measurement," in *Proc. IEEE Int. Instrum. Meas. Technol. Conf. (IMTC)*, May 2014, pp. 257–261.

[18] A. Ferrero and G. Superti-Furga, "A new approach to the definition of power components in three-phase systems under nonsinusoidal conditions," *IEEE Trans. Instrum. Meas.*, vol. 40, no. 3, pp. 568–577, Jun. 1991.

Sergio Toscani (S'08–M'12) received the M.Sc. (*cum laude*) and Ph.D. degrees in electrical engineering from the Politecnico di Milano, Milan, Italy, in 2007 and 2011, respectively.

Since 2011, he has been an Assistant Professor in electrical and electronic measurement with the Dipartimento di Elettronica, Informazione e Bioingegneria, Politecnico di Milano. He has authored or co-authored over 60 scientific papers. His current research interests include the development and testing of current and voltage transducers, measurement techniques for powers systems, electrical components, and systems diagnostics.

Dr. Toscani is a member of the IEEE Instrumentation and Measurement Society and the TC-39 - Measurements in Power Systems.

Carlo Muscas (M'98) received the B.S. degree in electrical, electronic and computer engineering and the M.S. (*cum laude*) degree in electrical engineering from the University of Cagliari, Cagliari, Italy, in 1994.

He was an Assistant Professor with the University of Cagliari from 1996 to 2001. Since 2001, he has been an Associate Professor of Electrical and Electronic Measurement with the University of Cagliari, where he is currently the Chairman of the Council for the B. S. degree in Electrical, Electronic and Computer Engineering. He has authored or co-authored over 130 scientific papers. His current research interests include the measurement of synchronized phasors, the implementation of distributed measurement systems for modern electric grid, and the study of power quality phenomena.

Mr. Muscas is currently an Associate Editor of the IEEE TRANSACTIONS ON INSTRUMENTATION AND MEASUREMENT.

Paolo Attilio Pegoraro (S'03–M'06) received the M.S. (*cum laude*) degree in telecommunications engineering and the Ph.D. degree in electronic and telecommunications engineering from the University of Padova, Padua, Italy, in 2001 and 2005, respectively.

He is currently an Assistant Professor of Electrical and Electronic Measurements with the Department of Electrical and Electronic Engineering, University of Cagliari, Cagliari, Italy. He has authored or co-authored over 70 scientific papers. His current research interests include the development of new measurement techniques for modern power networks, with particular attention to synchronized measurements, and state estimation for distribution grids.

Dr. Pegoraro is a member of the IEEE Instrumentation and Measurement Society and the TC-39 - Measurements in Power Systems.